Forest Chemicals Revew
www.forestchemicalsreview.com
ISSN: 1520-0191
July-August 2021 Page No. 1342-1354
Article History: Received: 12 May 2021 Revised: 25 June 2021 Accepted: 22 July 2021 Publication: 31 August 2021

Study on Structure and Remaining Oil Distribution Characteristics in Area 12 of Weigang

Liyan Sun[1], Zhiyuan Guo[1], Jicheng Zhang[1], Jia Niu[2]
[1]Department of Petroleum Engineering, Northeast Petroleum University; Key Laboratory of Enhanced Oil Recovery, Ministry of Education, China
[2]Department of Petroleum Engineering, Northeast Petroleum University, China

Abstract:

Through research, the occurrence and distribution law of faults are determined, the causes of complex fault block groups and the distribution characteristics of remaining oil are studied, and the development effect of complex fault block reservoirs is improved. The geological conditions of Weigang Oilfield, especially the characteristics of fault structures, are extremely complex. Determine the types and combination styles of faults, restore micro-geological structures as accurately as possible, and clarify the distribution of underground surplus resources.

***Keywords**: Complex Fault, Fault Identification, Remaining Oil.*

I. GEOLOGICAL SURVEY

Nanxiang basin is a Mesozoic-Cenozoic superimposed rift type oil-gas basin developed in the East Qinling fold belt, and Nanyang sag is a secondary structural unit of Nanxiang basin. Nanyang sag is divided into two structural zones with different characteristics, the south sag can be divided into three local structural zones: Tanggang-Gaozhuang fault anticline structural zone, Donnan fault structural zone, Niusanmen sag zone, Weigang-Beimazhuang fault nose structural zone and Dongzhuang sag zone. Weigang Oilfield is located in Weigang-Beimazhuang fault nose structural belt.

The target blocks in this study area are Wei i and ii fault blocks in Weigang Oilfield. Structure location: 1) South of No.1 fault, on the Weigang-Beimazhuang fault nose structural belt in the south of Nanyang sag, the reservoir type is a complex fault block oil field with structural-lithologic reservoirs, and the lithology is mainly siltstone and fine sandstone [1-3].

Forest Chemicals Revew
www.forestchemicalsreview.com
ISSN: 1520-0191
July-August 2021 Page No. 1342-1354
Article History: Received: 12 May 2021 Revised: 25 June 2021 Accepted: 22 July 2021 Publication: 31 August 2021

II. STRUCTURAL CHARACTERISTICS

Nanyang sag belongs to a relatively independent faulted structural unit in Nanxiang basin. Nanxiang basin is located in Qinling orogenic belt. It is a Mesozoic-Cenozoic continental oil and gas-bearing faulted basin developed in the late Yanshan period, and has experienced two development periods: faulted depression and depression. The basin is divided into Qinling fold belt and Dabie Mountain fold belt, which are intermountain fault basins. The periphery of the basin is controlled by faults. The total area of Nanxiang basin is 17000km^2, including Biyang, Nanyang and Xiangzao depressions [4,5].

There are more than 80 faults in Weigang Oilfield, including 6 main faults. According to the relationship between cross-section dip and general stratigraphic dip, the main faults in this area can be divided into two types: reverse normal faults and co-directional normal faults. The division of syndromic and reverse faults is of special significance [6]. Syndromic faults may change the occurrence of strata, make the strata dip in the faults opposite to the original, and the high point of fault block traps will move to the dip direction of the general strata dip. Reverse fault will not change the inclination of strata, so the high point of fault block trap is still in the upward dip direction of strata. Both of them play an important role in guiding the deployment of high-yield oil wells [7-9].

2.1 Fault Identification and Combination

Using orthogonal tangent to identify faults, according to fault anomaly analysis and preliminary interpretation of horizons, cut any line along the direction perpendicular to the fault, and find the breakpoint position. Multi-section tangents are used to analyze other tangents parallel to this arbitrary line, and orthogonal tangents are used to identify and implement low-order faults. Observe the strike of fault through continuous seismic profile, and identify the size and extension direction of fault [10,11]. (figure 1).

Forest Chemicals Revew
www.forestchemicalsreview.com
ISSN: 1520-0191
July-August 2021 Page No. 1342-1354
Article History: Received: 12 May 2021 Revised: 25 June 2021 Accepted: 22 July 2021 Publication: 31 August 2021

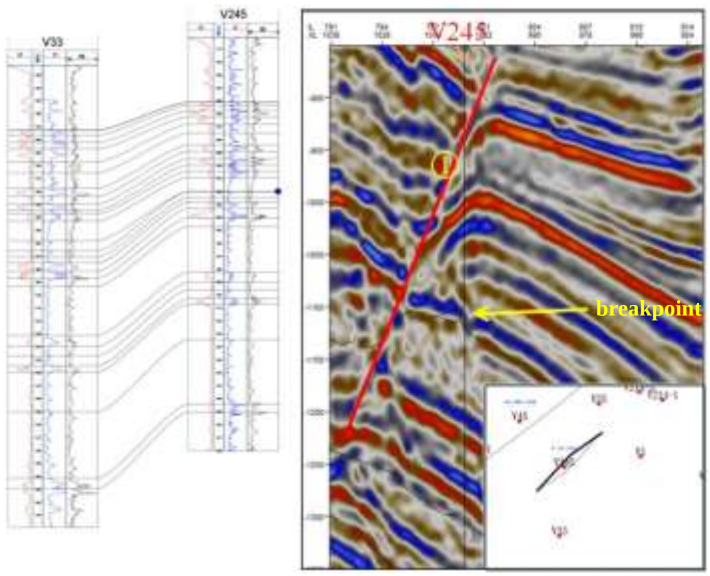

Fig 1: combination method of well seismic and orthogonal tangent fault

There are 64 large and small faults in Area 1-2 of Weigang Oilfield in Nanyang Sag, all of which are tensile faults, and their strike is mainly in the northeast and northwest directions. The cutting action divides a complete structure into many fault blocks. In each fault block (that is, one side of the section), the relationship between the interfaces of various strata is relative, and the thickness is stable or gradual. However, between different fault blocks (i.e., on both sides of the section), according to the height relationship and thickness change of the same stratum interface, the breakpoints of the same fault can generally be combined [12,13].

There are four main types of fault association relations in the depression: Y-shaped association, anti-Y-shaped association, Y-and anti-Y-shaped compound type and stepped type. (figure 4) The plane combination is zigzag, horsetail or broom, parallel and echelon. Y-shaped combination is the result of oblique shear and gravity on the stratum above shovel-shaped fault. The secondary fault intersects with the boundary fault in reverse, and is often associated with rollover anticline (Figures 2a and 3). This kind of assemblage develops in the central depression zone. The inverted Y-shape is caused by the joint action of the rotation of the section itself and the gravity of the overlying strata [14]. The inverted Y-shape is formed by the intersection of the secondary syncline fault and the boundary fault (Figures 2b and 3). The main fault plane is slow and the secondary fault plane is steep, which is easy to form a broken nose structure. This kind of assemblage develops in Weigang nose structural belt. Step-like fault combination is a series of profile representations of lateral or overlapping oblique faults with consistent strike and similar inclination (Figure 2c). This kind of assemblage is developed in the south of the depression, the northeast of the fault belt and Zhangdian nose structural belt.

Forest Chemicals Revew
www.forestchemicalsreview.com
ISSN: 1520-0191
July-August 2021 Page No. 1342-1354
Article History: Received: 12 May 2021 Revised: 25 June 2021 Accepted: 22 July 2021 Publication: 31 August 2021

The "Y" and anti-"Y" compound type is easy to form broken anticline and broken nose structures, and its plane combination is broom-shaped, and the order of all levels on the section is clear (Figure 2d), and this kind of combination is relatively developed in the transition area of uplift and depression. There is a Y-type combination pattern between No.1 fault and No.2 fault in the study area [15]. Through fault combination, it is found that Weigang Oilfield is dominated by Y-type combination fault and anti-Y-type combination model (Figures 3 and 4). Thereby establishing a three-dimensional spatial combination model of faults in the target stratum in the study area (Figure 5) [16].

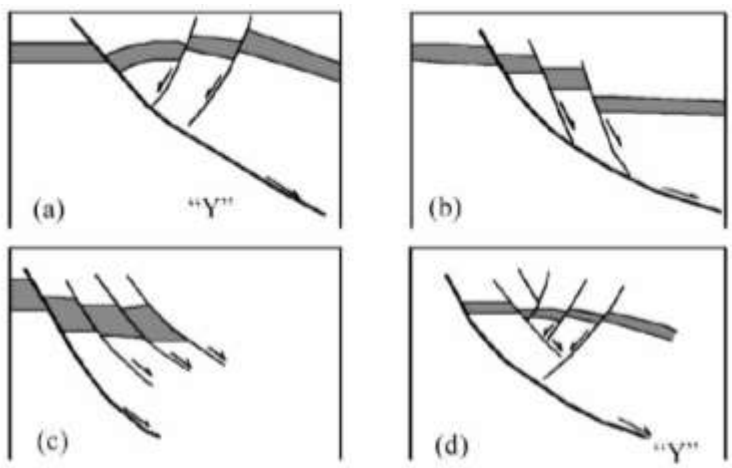

(a) Y-type combination (b) anti-Y-type combination

(c) stepped fracture combination (d) Y-type and anti-Y-type composite combination.

Fig 2: combination style of fault section in Nanyang sag

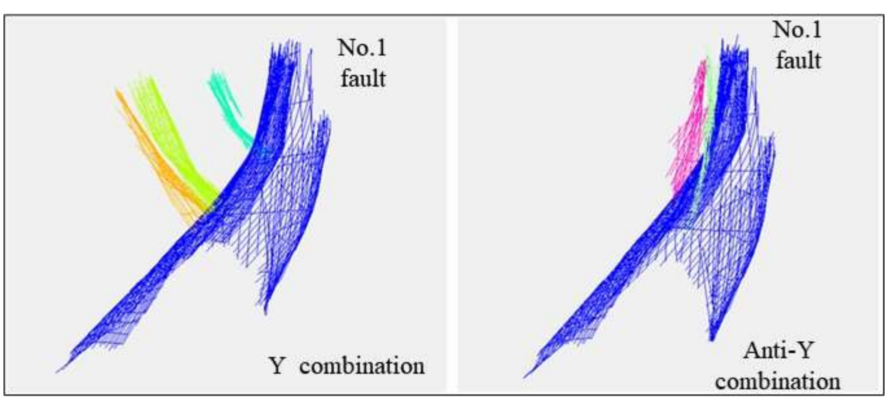

Forest Chemicals Revew
www.forestchemicalsreview.com
ISSN: 1520-0191
July-August 2021 Page No. 1342-1354
Article History: Received: 12 May 2021 Revised: 25 June 2021 Accepted: 22 July 2021 Publication: 31 August 2021

Fig 3: fault combination model

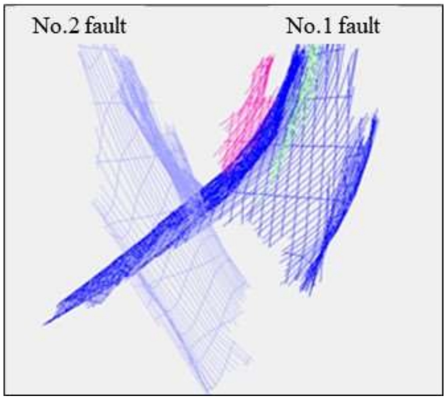

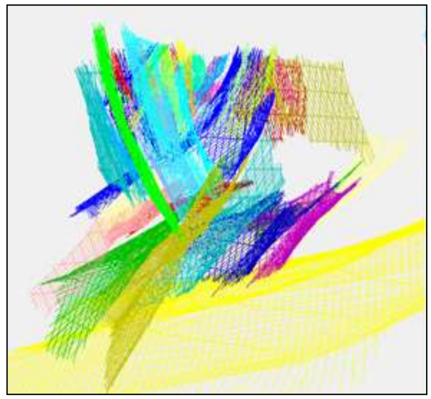

Fig 4: Y-type combination model of No.(1) fault and No.(2) fault
Fig. 5 fault combination model of Weigang Oilfield

2.2 Influencing Factors and Genetic Types of Complex Fault Groups

The causes of the deformation of the Weigang nose structure fault are mainly related to three factors, namely, the mantle uplift, the change and distribution of the overburden properties, and the later tectonic movement.

I. Mantle uplift is related to lithospheric stretching and thinning.

II. It is related to uneven distribution of lithology, differential compaction and gravity. In the sand-mud alternating zone, normal faults are easy to form due to differential compaction, and the load of overlying strata promotes the formation and activity of faults.

Complex fault block group is a three-dimensional structural combination caused by long-term tectonic evolution, and its origin mainly depends on the geometric shape of main basement faults and boundary faults of fault blocks and their mutual cutting relationship. On the one hand, the displacement of the main basement fault causes the deformation of its two fault blocks and changes the local stress state; On the other hand, it induces the development of secondary regulating faults, leading to the development of different types of complex fault block groups. Therefore, the geometric shape and movement mode of the main basement faults not only control the basic structural characteristics of the basin, but also control the formation and evolution of complex fault block groups with different characteristics [17,18].

In the graben formed by two opposite main faults, the graben blocks are further cut into fault steps and grabens due to the development of the sequence of their respective derived

Forest Chemicals Revew
www.forestchemicalsreview.com
ISSN: 1520-0191
July-August 2021 Page No. 1342-1354
Article History: Received: 12 May 2021 Revised: 25 June 2021 Accepted: 22 July 2021 Publication: 31 August 2021

faults or later faults. On the plane, the boundary main faults of the graben are nearly parallel, or oblique or argumentative, while the No.1 fault and No.2 fault are nearly parallel in the main area (Figure 6), and the internal secondary faults are generally parallel to their control faults. On the profile, a secondary graben is generally formed in the middle of the graben, while fault steps are formed on both sides, and the strata are gradually lowered from both sides to the middle (Figure 7). This kind of fault block group is mainly developed in the main fault drop plate inside the depression [19-21].

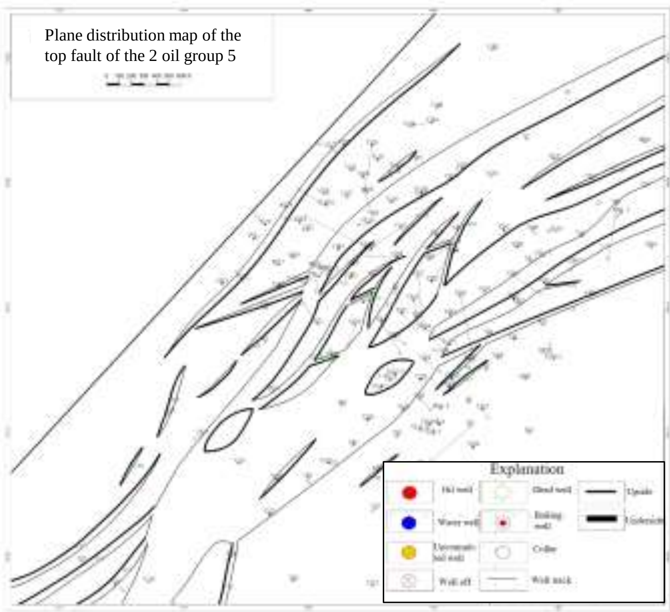

Fig 6: plane distribution characteristics of complex fault block groups of compound graben type

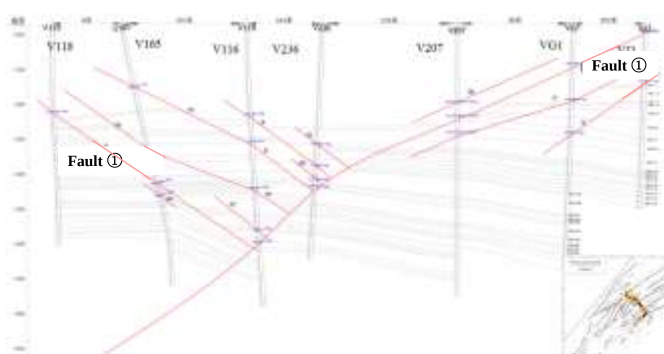

Fig 7: distribution characteristics of vertical faults in complex fault block groups of compound graben type

Forest Chemicals Revew
www.forestchemicalsreview.com
ISSN: 1520-0191
July-August 2021 Page No. 1342-1354
Article History: Received: 12 May 2021 Revised: 25 June 2021 Accepted: 22 July 2021 Publication: 31 August 2021

III. STUDY ON THE DISTRIBUTION OF REMAINING OIL IN AREA 1-2 OF WEIGANG

3.1 Fine Geological Modeling

3.1.1 Establish the model

Based on the imported fault data, the fault model of the work area is established, and the fault trend in the work area is mainly NNW. According to the actual situation of work area, well pattern density and so on, the plane step length of a single grid is 10m×10m, and the number of plane grids is 595× 340. There are 22 sedimentary units in the vertical direction, and finally the number of grids in three directions is 595×340×22.

The model of permeability and effective thickness is established with phase model as constraint, and the algorithm adopted is sequential Gaussian model. Attribute modeling mainly consists of three steps: attribute discretization, data analysis and attribute modeling [22].

3.1.2 Numerical simulation

The fluids in the strata in the study area mainly include oil and water phases. The basic reservoir parameters mainly include original formation pressure, high-pressure physical properties of rocks, water and crude oil, etc. Numerical simulation of basic reservoir parameters such as high-pressure physical properties of rocks and fluids mainly refers to coring well data and laboratory experiment results, as shown in Table I [23].

TABLE I. Basic reservoir parameter table for numerical simulation of oil layer in the study area

PARAMETER	DATUM DEPTH(M)	PRESSURE CORRESPONDING TO DATUM DEPTH(BAR)	SATURATION PRESSURE OF CRUDE OIL(BAR)	CRUDE OIL DENSITY(G/CM^3)	CRUDE OIL FORMATION VISCOSITY(MPA·S)	CRUDE OIL VOLUME COEFFICIENT	COMPRESSION COEFFICIENT OF CRUDE OIL(1/BAR)	FORMATION WATER COMPRESSION COEFFICIENT(1/	ROCK COMPRESSION COEFFICIENT(1/BAR)

Forest Chemicals Revew
www.forestchemicalsreview.com
ISSN: 1520-0191
July-August 2021 Page No. 1342-1354
Article History: Received: 12 May 2021 Revised: 25 June 2021 Accepted: 22 July 2021 Publication: 31 August 2021

								BAR)	
VALUE	1300	142	100	0.852	8.3	1.1	1.0×10^{-5}	1.1×10^{-5}	6.0×10^{-6}

3.2 Reservoir heterogeneity in area 1 and 2 of Weigang oilfield

According to the static characteristics of Area 1-2 of Weigang Oilfield, reservoir attribute modeling is established, including porosity model and permeability model. According to Table II, the permeability of the whole region is unevenly distributed, with an average permeability of 53mD and a coefficient of variation of permeability of 0.81, with strong heterogeneity. Vertically, the coefficient of variation of permeability of each layer is between 0.7 and 0.95, and the difference between layers is serious. Among them, the sand bodies are well developed, the oil-bearing area is large, and the layers with good physical properties are H2I1, H2II10 and H2II15 [24,25].

TABLE II. Physical parameters of each layer

ANALOG LAYER SERIAL NUMBER	ACTUAL FLOOR NUMBER	ORIGINAL RESERVES(10^4T)	INITIAL OIL SATURATION	POROSITY	PERMEABILITY(MD)	STANDARD DEVIATION	VARIABLE COEFFICIENT
1	H2I1	40.2	0.7300	0.2244	135	97	0.72
2	H2I2	7.06	0.6720	0.2027	103	84	0.82
3	H2I3	4.83	0.7189	0.1736	82	70	0.85
4	H2I4	3.41	0.7532	0.2069	108	91	0.84
5	H2II5-6	32.51	0.7398	0.2107	118	99	0.84
6	H2II7	21.34	0.6857	0.1861	116	93	0.80
7	H2II8-9	35.86	0.6833	0.1924	120	101	0.84

Forest Chemicals Review
www.forestchemicalsreview.com
ISSN: 1520-0191
July-August 2021 Page No. 1342-1354
Article History: Received: 12 May 2021 Revised: 25 June 2021 Accepted: 22 July 2021 Publication: 31 August 2021

8	H2II10	81.45	0.7106	0.2345	103	82	0.80
9	H2II11	13.4	0.6411	0.1974	103	91	0.88
10	H2II12	44.74	0.7229	0.2311	148	101	0.69
11	H2II13	6.14	0.7110	0.1994	131	106	0.81
12	H2II14	17.18	0.6910	0.2353	124	99	0.80
13	H2II15	80.43	0.7324	0.2125	101	95	0.94
14	H2III16-19	34.78	0.7330	0.2062	106	87	0.82
15	H2III20	4.85	0.6629	0.2302	118	82	0.70
16	H2III21	12.09	0.7418	0.1719	97	82	0.85
17	H2III22	23.78	0.7483	0.1911	114	95	0.83
18	H2III24	19.09	0.6508	0.1547	84	72	0.85
19	H2III25-27	83.28	0.6979	0.2289	82	74	0.90
20	H2III30	9.01	0.6690	0.2338	78	74	0.95
全区		575.43	0.7151	0.2019	112	112	0.81

3.3 Distribution Characteristics of Remaining Oil

The influence of sedimentary environment and sedimentary microfacies of sand body shape, different oil layer properties, different production degree and different remaining oil enrichment degree. Therefore, according to the permeability and oil saturation, the distribution of remaining reserves in each sedimentary unit is counted [26]. (Figure 8, Figure 9).

Forest Chemicals Review
www.forestchemicalsreview.com
ISSN: 1520-0191
July-August 2021 Page No. 1342-1354
Article History: Received: 12 May 2021 Revised: 25 June 2021 Accepted: 22 July 2021 Publication: 31 August 2021

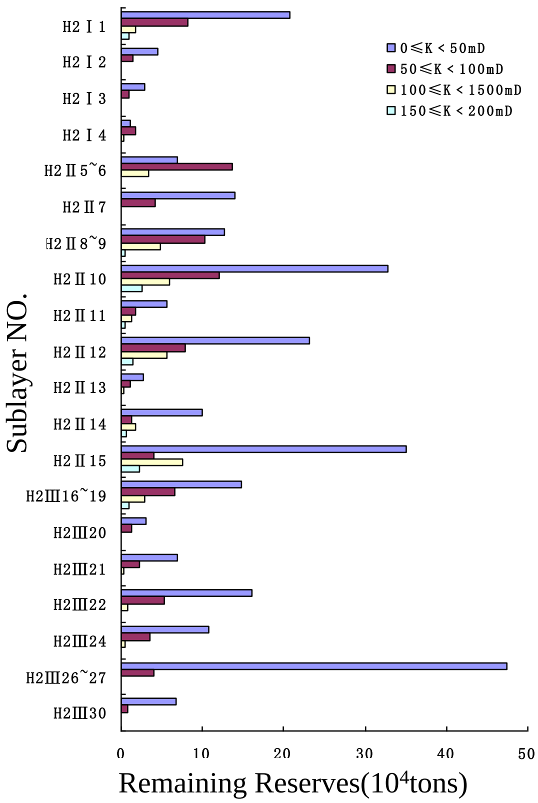

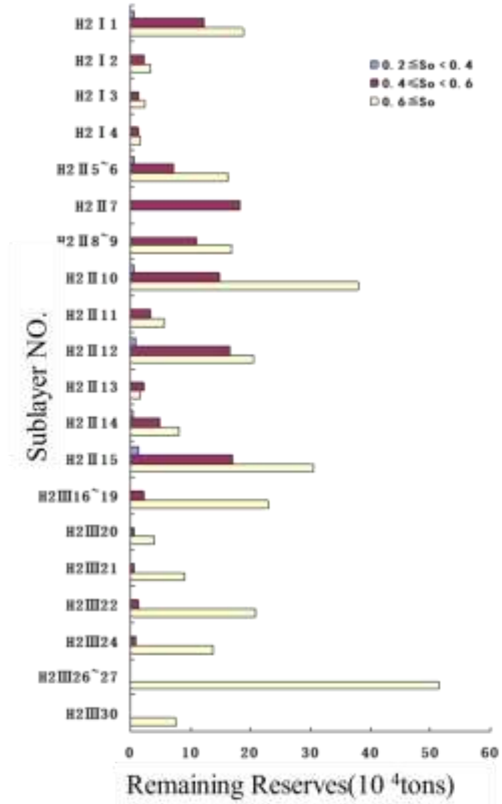

Fig 8: remaining reserves in different permeability regions
Fig 9: remaining reserves in different oil saturation areas

Among the remaining reserves in permeability classification statistics, the remaining reserves with permeability in the range of 0 MD to 50 MD are 2,779,400 tons, accounting for the largest proportion, accounting for 66.66% of the regional remaining reserves. However, the remaining reserves in the permeability range of 150 MD to 200 MD are 103,000 tons, accounting for 2.47% of the regional remaining reserves. The remaining reserves in the numerical model area tend to decrease with the increase of permeability. It shows that the water flooding effect of high permeability layer is good and the remaining oil potential is small. The remaining oil is mainly distributed in low permeability areas [27-29].

In the oil saturation classification statistics of remaining reserves, the remaining reserves in the range of So ≥ 0.6 are 2,945,200 tons, accounting for 70.71% of the regional remaining reserves, which is the main target for tapping the potential of remaining oil. However, the remaining reserves in areas with oil saturation between 0.2 and 0.4 are only 5.48, accounting for 1.32% of sedimentary units. The remaining oil is not enriched in the area where so is less

Forest Chemicals Revew
www.forestchemicalsreview.com
ISSN: 1520-0191
July-August 2021 Page No. 1342-1354
Article History: Received: 12 May 2021 Revised: 25 June 2021 Accepted: 22 July 2021 Publication: 31 August 2021

than 0.2. Therefore, the middle and high oil saturation areas should be the main targets for tapping the potential of remaining oil.

IV. CONCLUSION

I. Fine contrast breakpoint identification technology: 2D and 3D linkage breakpoint identification, establishing 3D breakpoint distribution map, improving the identification accuracy of spatial breakpoints, and completing the whole area identification work. Identification of faults and combined faults by using seismic data-aided detection technology.

II. Establish the geological model and fault model of the study area, and complete the structural modeling, porosity, permeability and original oil saturation model according to the logging curve. The actual geological reserve of the numerical model in the study area is 579.22×104t, and the fitted geological reserve is 575.43×104t Complete the production dynamic fitting of the whole area and single well, and the fitting indexes include water cut, oil production, liquid production and water injection, etc. The permeability of the whole region is unevenly distributed, with an average permeability of 113mD and a permeability variation coefficient of 0.81, with strong heterogeneity. Vertically, the coefficient of variation of permeability of each layer is between 0.65 and 0.95, and the difference between layers is serious. Among them, the sand bodies are well developed, the oil-bearing area is large, and the layers with good physical properties are H2I1, H2II10 and H2II15.

III. The formation and distribution of remaining oil in the study area are mainly controlled by sedimentary facies, structure, reservoir heterogeneity and well pattern conditions. The remaining oil is mainly controlled by fault area and imperfect injection and production.

REFERENCES

[1] Wu D, Wu Z, Wu Y (2020) A new method for high resolution well-control processing of post-stack seismic data - ScienceDirect. Natural Gas Industry B 7(3):215-223
[2] Bychkov S, Mityunina IY, Perm, et al. (2015) Near-Surface Correction on Seismic and Gravity Data. (6):7
[3] Zhang Y, Lin H, Li Y, et al. (2020) Seismic Signal Enhancement and Noise Suppression Using Structure-Adaptive Nonlinear Complex Diffusion. IEEE Transactions on Geoscience and Remote Sensing 58(3):2198-2211
[4] Hou G, Feng D, Wang W (2004) Reverse structures and their impacts on hydrocarbon accumulation in Songliao basin. Oil and Gas Geology, 25(1):49-53

[5] Lei Q, Yun XU, Yang Z, et al. (2021) Progress and development directions of stimulation techniques for ultra-deep oil and gas reservoirs. Petroleum Exploration and Development 48(1):11

[6] Shi ZM, Bai QY, Hui JW (2005) Oil and Gas Accumulation Mechanism and Model of Putaohua Oil Layer in Sanzhao Depression. Daqing:School of Earth Sciences, Daqing Petroleum Institute: 20-80.

[7] Wei LA, Xw A, Bz B, et al. (2020) Large-scale gas accumulation mechanisms and reservoir-forming geological effects in sandstones of Central and Western China. Petroleum Exploration and Development 47(4):714-725

[8] Jia FQ, Yi PX, Qiao Y (2004) Structural analysis of oil zone. Petroleum Industry Press: 25-59

[9] Wen CZ (1991) Logging Evaluation Technology for Oil and Gas Reservoir. Petroleum Industry Press

[10] Liu Y, Li JR, Yan RH, et al. (2020) A New Method for Rapid Identification of Tight Oil Reservoir Fluid Property Logging in the Foreland Basin on the Southwestern Margin of Ordos Basin

[11] AMW, ADJ, BAL, et al. (2013) Late Holocene activity and historical earthquakes of the Qiongxi thrust fault system in the southern Longmen Shan fold-and-thrust belt, eastern Tibetan Plateau. Tectonophysics 584(1):102-113

[12] Granado C, Muoz-Martín A, Olaiz AJ, et al. (2021) 3D crustal-scale structure of the West Iberia margin: a novel approach to integrated structural characterization of passive margins. Marine Geophysical Research 42(2):1-30

[13] Mikkelsen PL, Guderian K, Plessis GD (2008) Improved Reservoir Management through Integration of 4D-Seismic Interpretation, Draugen Field, Norway. Society of Petroleum Engineers Reservoir Evaluation & Engineering 2:9~17

[14] Cindy P, Radmila Pe, Maj W, etc. (2009) Integration of High Resolution 3D Seismic and Long Horizontal Well Data for Predictive Structural Modeling of the Tight Cretaceous Kharaib B Reservoir in the AI Shaheen Field, Offshore Qatar. International Petroleum Technology Conference, Doha, Qatar 12(7~9):1~4

[15] Min W (2013) Research on the Technical Policy Boundary of Middle-Deep and Low-Permeability Reservoir Development. Yangtze University

[16] Huo J, Shi GX (2010) The Horizontal Well Production Technique with Thin Bedded Bottom Water Reservoir in Luliang Oil Field. SPE131890

[17] Yu W (2010) Evaluation of remaining oil potential and production status of various oil layers in Sazhong Development Area. Daqing Petroleum Institute

[18] He F (2016) Tapping the potential countermeasures for stabilized production in Bozhong 34-1 Oilfield. Mud Logging Engineering

[19] Shao KZ (2011) Research on the Production Status of Sandbody Reserves in the Developed Blocks of Satellite Oilfield. Northeast Petroleum University

[20] Zeito GA Interbedding of Shale Breaks and Reservoir Heterogeneities, JPT. 1065(10): P1223-1228

[21] Yan G, Rui S, Fang Z, et al. (2013) Research on Waterflood Sweep Law in Low Permeability Vertical Heterogeneous Reservoir. International Journal of Digital Content Technology and its Applications 7(6):698-705

[22] Kuzmina S, Rosneft, Butula KK (2009) Reservoir Pressure Depletion and Water Flooding Influencing Hydraulic Fracture Orientation in Low-Permeability Oilfields. SPE120749

[23] Guo FZ, Tang H, Dong Liang LV, et al. (2011) Research on rational formation pressure maintenance level in low permeability reservoir. Special Oil & Gas Reservoirs 18(1):90-92

Forest Chemicals Revew
www.forestchemicalsreview.com
ISSN: 1520-0191
July-August 2021 Page No. 1342-1354
Article History: Received: 12 May 2021 Revised: 25 June 2021 Accepted: 22 July 2021 Publication: 31 August 2021

[24]Xin W (2013) Research on the Technical Policy Boundary of Thin and Poor Reservoir Development. Northeast Petroleum University
[25] Cong L, Li WL, Lei JC, et al. (2013) The Current Situation and Prospects of Development of Low Permeability Oil Reservoir. Advanced Materials Research
[26] Liu Y, Wu X, Zhai X, et al. (2020) The research status and summary of adsorption and retention mechanism of polymer. IOP Conference Series: Materials Science and Engineering 892(1): 012023 (7pp)
[27] Feng M (2008) Planar grid division of the numerical simulation of remaining oil distribution during high water-cut period. Petroleum Geology and Recovery Efficiency
[28] Li Z, Wollen C, Yang P (2008) Potential Use of Produced Oil Sample Analysis to Monitor SAGD Performance. International Thermal Operations and Heavy Oil Symposium 20:1-16
[29] Ji CZ, Yan HZ, Fei Z (2010) Study on the distribution of remaining oil potential in oilfield after polymer flooding. Mathematics practice and knowledge 7: 531-534